Int J Adv Manuf Technol (2014) 73:353–364
DOI 10.1007/s00170-014-5828-1

ORIGINAL ARTICLE

Measurement and evaluation of surface roughness based on optic system using image processing and artificial neural network

Gürcan Samtaş

Received: 26 November 2013 / Accepted: 31 March 2014 / Published online: 18 April 2014

Abstract The traditional devices, used to measure the surface roughness, are very sensitive, and they are obtained by scratching the surface of materials. Therefore, the optic systems are used as alternatives to these devices to avoid the unwanted processes that damage the surface. In this study, face milling process was applied to American Iron and Steel Institute (AISI) 1040 carbon steel and aluminium alloy 5083 materials using the different tools, cutting speeds and depth of cuts. After these processes, surface roughness values were obtained by the surface roughness tester, and the machined surface images were taken using a polarise microscope. The obtained images were converted into binary images, and the images were used as input data to train network using the MATLAB neural network toolbox. For the training networks, log-sigmoid function was selected as transfer function, scaled conjugate gradient (SCG) algorithm was used as training algorithm, and performance of the trained networks was achieved as an average of 99.926 % for aluminium alloy (AA) 5083 aluminium and as an average of 99.932 % for AISI 1040 steel. At the end of the study, a prediction programme for optical surface roughness values using MATLAB m-file and GUI programming was developed. Then, the prediction programme and neural network performance were tested by the trial experiments. After the trial experiments, surface roughness values obtained with stylus technique for the carbon steel and aluminium alloy materials were compared with the developed programme values. When the developed programme values were compared with the experimental results, the results were confirmed each other at a rate of 99.999 %.

Keywords Surface roughness prediction · Optical technique · Stylus technique · Image analysis

G. Samtaş (✉)
Engineering Faculty, Department of Mechatronics, Düzce University, 81620, Beci Yorukler Düzce, Turkey
e-mail: gurcansamtas@duzce.edu.tr

1 Introduction

Surface quality is an important indicator of the engineering material quality, and the main indicator of the surface quality of the machined workpieces is surface roughness. The accurate measurement of the surface roughness is of great importance for the area of the precision engineering and manufacturing industry. Surface roughness is commonly measured mechanically with a stylus device [1–3]. For many years, the stylus device has been widely used for measuring surface roughness parameters with high reliability. The vertical movement of tip of the stylus is measured for a prespecified length horizontally. The stylus tip, however, could not reach into all the valleys of the surface [4]. On the other hand, the conventional method for measuring surface roughness is to pass a stylus probe across the surface and to monitor its movement such that the surface micro-profile can be traced. These devices are very sensitive. However, some of them, such as the diamond stylus, could scratch the surface, particularly when the material is soft [5]. Measurements using the stylus technique (contact system) can damage the surface because it contacts the material surface, and this technique is suitable only for point measurement. Therefore, the instrument must be handled carefully in a fairly clean environment. Another problem with the stylus measurement technique is the size of the stylus radius and the crevices on the surface. If the crevices are narrow such that the stylus cannot penetrate all the way to the bottom, the measurement will not be accurate and a true representation of the surface [6]. Accordingly, measuring of the surface roughness with optical systems (non-contact) can eliminate these problems [7–10]. Although there are many methods using the optical systems to measure the surface roughness, new methods are also being developed to eliminate the faced problems.

Some researchers have worked in the area of classification and assessment of textures using machine vision in the past

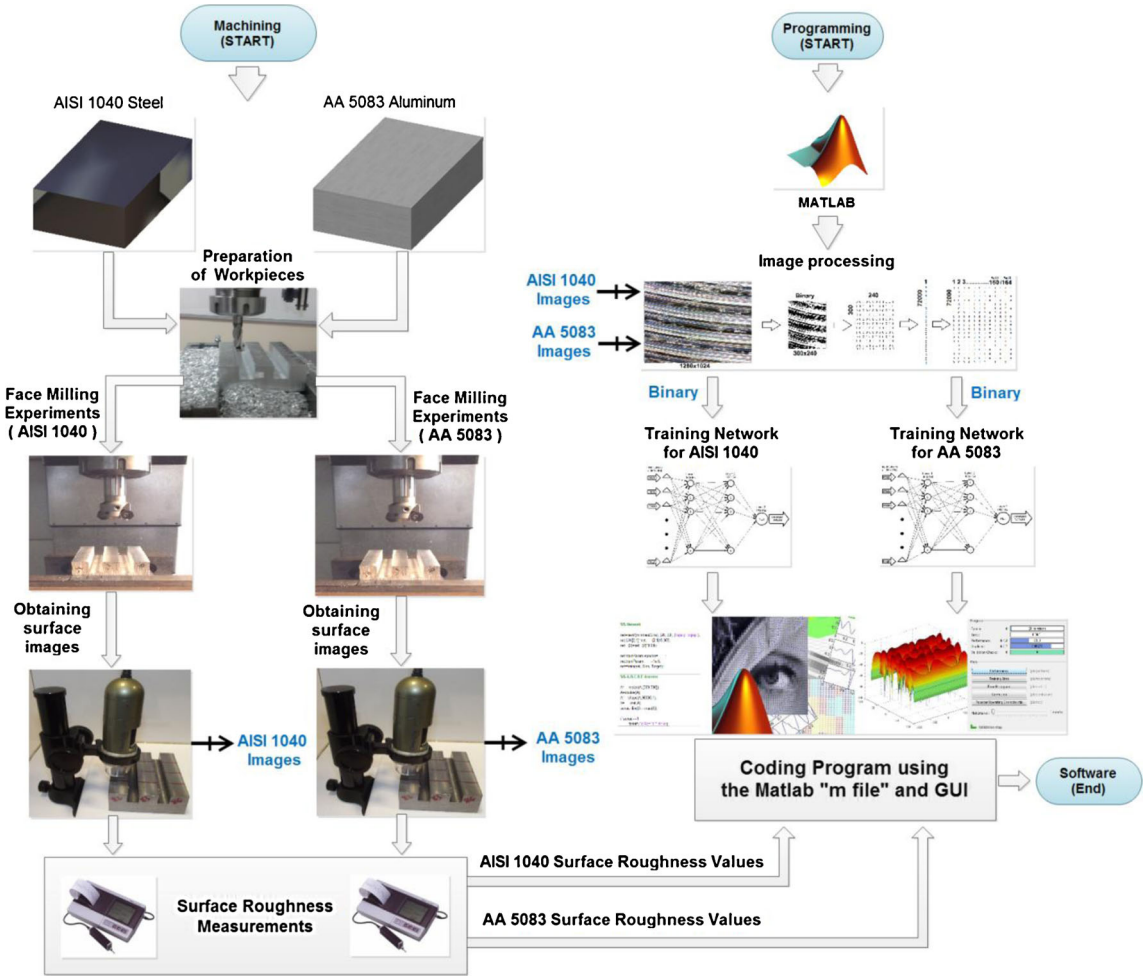

Fig. 1 Flow chart of experimental set-up, captured image and programming section

years [11–13]. Dhanasekar and Ramamoorthy [5] grabbed the images using a vision system and evaluated the statistical roughness parameters of image textures as spatial frequency and arithmetic average of grey level. Then, these parameters were used as input values to train neural network. The surface roughness values obtained from training network were compared with the stylus roughness values [5]. Tsai et al. [14] assessed the surface roughness of machined parts produced by the shaping and milling processes and extracted features of surface roughness in the spatial frequency domain using the 2D Fourier transform. These roughness features were taken as input to artificial neural networks (ANNs) to categorise the surface of interest among a set of standard surfaces of known roughness values.

The application of dynamic speckle technology has been mostly focused on the measurements. A speckle pattern image

Table 1 The selected cutting parameters for face milling process

Materials	Parameters	Levels		
		1	2	3
AISI 1040	Cutting depth (mm)	0.3	0.6	0.9
	Cutting tools (coated/uncoated)	Uncoated	TiN-TiCN-Al_2O_3	TiAlN
	Cutting speed (m/min)	160	180	220
	Feed rate (mm/tooth)	0.10	0.15	0.30
AA 5083	Cutting depth (mm)	0.08	0.12	0.25
	Cutting tools (coated/uncoated)	Uncoated	TiAlN	TiB_2
	Cutting speed (m/min)	450	550	650
	Feed rate (mm/tooth)	0.08	0.12	0.25

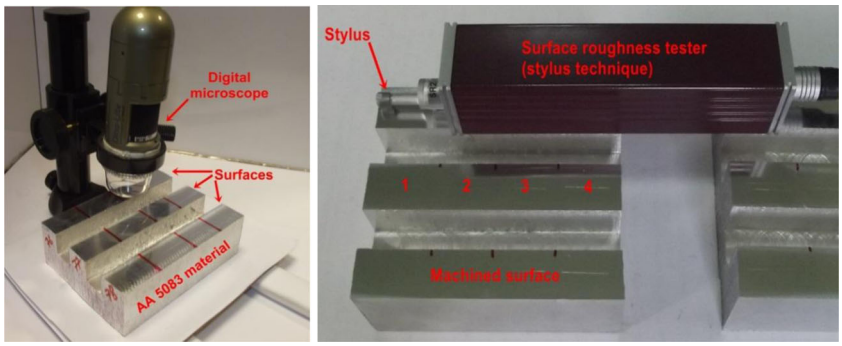

Fig. 2 Taking photos and surface roughness measurements

is generally obtained from a He-Ne laser beam. It is produced from a stationary surface carrying the micro-structure information of the surface and can be recorded in image for prediction of surface roughness [15]. Fuh et al. [16] developed a method of intensity distribution of binary image and an adaptive optics integrated system for measuring the surface roughness under dynamic turbulence. Hamed et al. [17] evaluated the object surface roughness of aluminium surfaces using a technique based on computing the signal to noise ratio of the obtained numerical speckle images. Kayahan et al. [18] presented the results from an optical technique for measuring surface roughness using image analysis of speckle pattern images. In this study, the speckle patterns obtained with a He-Ne laser were binarised and analysed. Persson [19] examined the measurement of surface roughness using an angular speckle correlation on machined surface, and a new technique to achieve increased repeatability by using an angle detection unit was presented. Meireles et al. [20] conducted an experimental investigation of speckle pattern formation from metallic surfaces at diffraction plane.

Many statistical and structural texture analysis methods were used for the evaluation of machined surfaces. In addition, first-, second- and higher-order statistical textural analyses were used to evaluate the quality of machined surfaces. One of the second-order statistical techniques is grey level co-occurrence matrix (GLCM) technique. This technique gives the information about the relative occurrence of pixel intensities between two pixels in a special spacing or pixel pair spacing and pixel pair direction. Moreover, GLCM can be used as an image analysis of surface texture of resulting machined surface images [21]. Gadelmawla [22] implemented a vision system to capture images for surfaces to be characterized and developed software to analyse the captured images based on the GLCM. Wang et al. [23] presented the grey reference line for surface roughness evaluation based on grey system theory. These techniques are a wide range of application of digital image processing, and it can be integrated and applied in many industrial applications [24–29].

The aim of this paper is to present an optical technique including statistical properties of binary image method [18, 30] to detect surface roughness values. This technique used the ANNs for the surface roughness measurement based on binary digitised images from a digital microscope on the face-milled surfaces of carbon steel and aluminium alloy. In this study, a total of 162 experiments were conducted with two materials for face milling process, and a total of 648 images, four images for each experiment, were taken using a digital microscope from the material faces (Fig. 1).

The captured images were converted into the binary images, which were used as input parameters to train neural networks using the logistic sigmoid curve and the scaled conjugate gradient method. At the end of this paper, a prediction programme was developed to obtain vision surface roughness values from the images, and trial experiments were performed to test performance of the prediction programme, comparing stylus values and vision surface roughness values. Coding of the prediction programme, image processing and training neural networks processes were conducted by MATLAB.

2 Experimental procedures

2.1 Machining of the materials

In this study, American Iron and Steel Institute (AISI) 1040 carbon steel and aluminium alloy (AA) 5083-H111-tempered aluminium alloy blocks were used as the workpiece materials. Uncoated, TiALN-coated, TiN-TiCN-Al_2O_3-coated and TiB_2-coated carbide cutting inserts were used in the experiments.

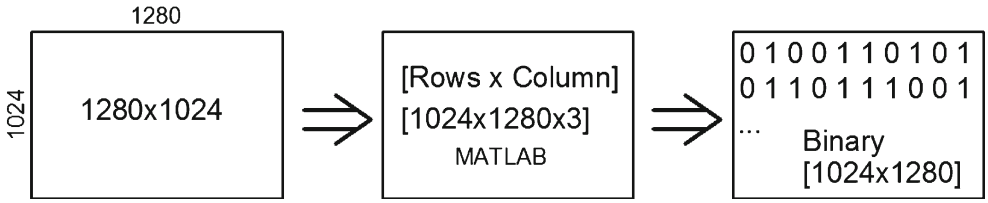

Fig. 3 Binary files converting using image processing toolbox

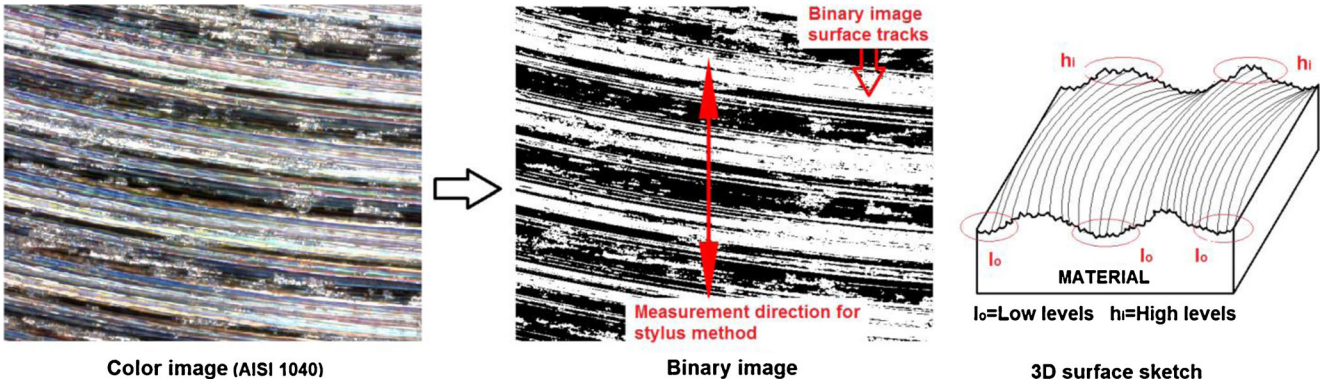

Fig. 4 Converting to binary image and experimental measurement direction for stylus method

Before the experiments, workpieces were created having three different machining faces and two channels in accordance with ISO 8688-1 using the end mill tool. Test specimens were prepared using the Jetco JVM-2 milling machine. The face milling experiments were performed using the first model MCV-300 three-axes CNC vertical machine centre (Fanuc Oi Mate MC) having a maximum spindle speed of 8,000 rpm, a pneumatic pressure of 5.5 bar and a 12-kW drive motor. To determine the cutting parameters for experimental procedures, manufacturer's data of cutting tool and the recommendations contained in the ISO 8688-1 standard were taken into consideration. The experiments, for the two selected materials, were conducted by using the parameters given in Table 1.

In this study, a total of 162 experiments were performed with two materials for face milling process using cutting parameters.

2.2 Captured images and surface roughness measurements

After experiments, surface images were taken from four different regions of machined surface using a digital microscope for each test, and then, surface roughness measurements were conducted by using a surface roughness tester using middle regions of the machined faces (Fig. 2). Total of 648 surface images of 1,280×1,024 resolution were obtained using the Dino-Lite Pro2 brand AMT413ZT model polarised microscope with a magnification of up to 240 times. The surface roughness of the machined faces was measured using a Mitutoyo portable surface roughness tester (Mitutoyo Surftest SJ-301, Product No. 99MBB035A1, Series No. 178; Mitutoyo Corporation, 20-1, Sakado 1-chome, Takatsu-ku, Kawasaki, Kanagawa 2002; 213-0012, Japan).

3 Image processing and training networks

The obtained images from the surfaces were analysed by MATLAB image processing toolbox. Neural network toolbox was also used to train the networks. Surface images were evaluated by the test programme coded using MATLAB m-file for different resolutions (800×640, 700×560, 500×400, 400×320, 240×300 and 300×240) as binary format. MATLAB can use all types of images by converting them to the matrix format. Therefore, these resolutions were evaluated for the maximum matrix size that can be handled by the programme during the training networks.

3.1 Image processing and creating matrices

A 1,280×1,024-resolution image corresponds to 1,280 horizontal and 1,024 vertical pixels on a computer display.

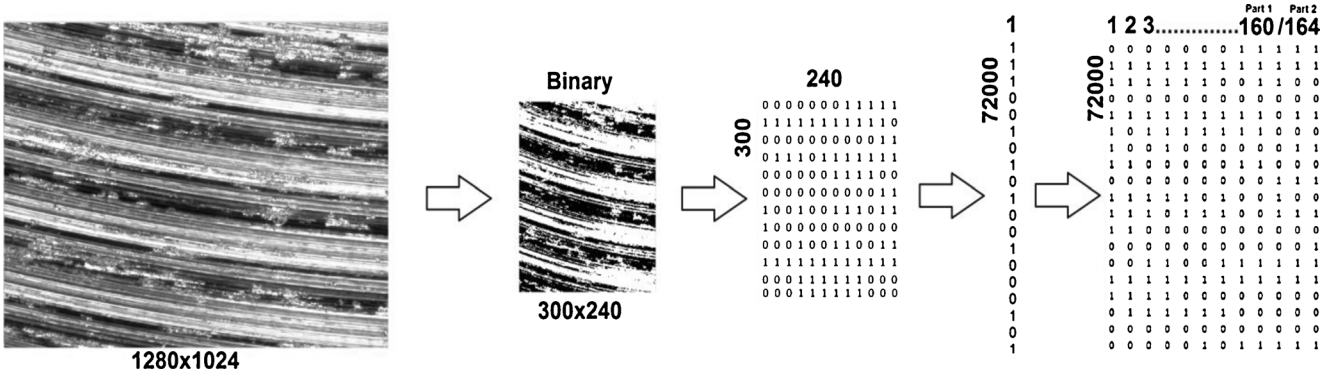

Fig. 5 Applied processes to images

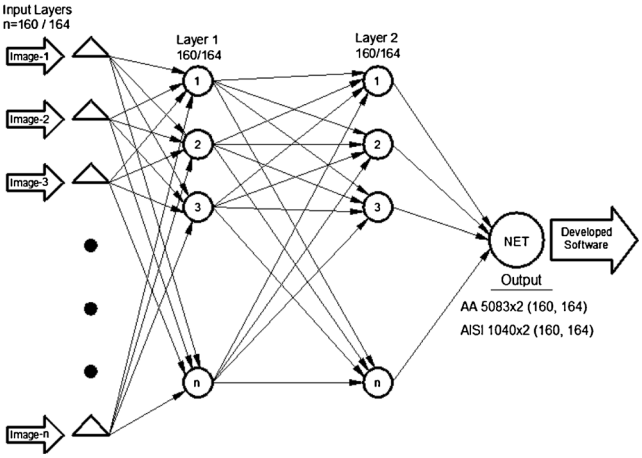

Fig. 6 Neural network structure for the processed images

However, this colour image is coded in MATLAB as red, green and blue (RGB) colour-coding system based on 1,024×1,280×3 (rows×columns×layer). In this study, the obtained images from the experiments were used by converting binary formats in MATLAB (Fig. 3).

The images converted to binary format, pixels in binary images with a value of 0, were displayed as black, and pixels with the value of 1 were displayed as white. In statistics, binary data is a statistical data type defined by binary variables, which can take only 0 and 1 as possible values. Statistical property modelling with the binary images could be effectively used for surface roughness, and it has a great potential in process measurements [18]. When the images defined in binary format are converted into two-dimensional matrices, a black and a white (B/W) image of 1,280×1,024 resolution will have 1,310,720 pixels that is a matrix units of 0 and 1.

In Fig. 4, the black areas on the binary image are the low levels that are created after the face milling process. The white areas define the high levels. The linear tracks in both material surfaces are formed due to the milling process. In experimental measurements, surface roughness measurement stylus was moved as perpendicular to these tracks. On the other hand, this direction was considered as an important criterion in terms of image processing for detecting fluctuations in the appropriate colour. Most of the non-contact methods are based on statistical methods and the other method, as Machine Vision System uses optical surface roughness features of the surface

Table 2 Neural network parameters for AA 5083 material

Transfer functions	Number of neurons	Training algorithms			
		SCG (R^2)	CGB (R^2)	GD (R^2)	CGF (R^2)
Logsig	50	0.02592	0.00099	0.00208	0.00717
	100	0.03855	0.56432	0.00053	0.23215
	125	0.97383	0.37929	0.00254	0.00113
	160	*0.99921*	0.00273	0.00172	0.50207
Radbas	50	0.67130	–	0.00632	–
	100	0.71367	–	–	–
	125	0.71459	–	0.00300	–
	160	0.66666	–	0.00117	–
Pureline	50	0.56077	0.55239	–	0.55480
	100	0.79305	0.78766	–	0.78461
	125	0.88313	0.87575	–	0.88199
	160	0.99647	0.95861	–	0.98206

Table 3 Neural Network parameters for AISI 1040

Transfer functions	Number of neurons	Training algorithms			
		SCG (R^2)	CGB (R^2)	GD (R^2)	CGF (R^2)
Logsig	50	0.43428	0.23630	0.00030	0.00156
	100	0.99829	0.51402	0.00440	0.00285
	125	0.99973	0.56010	0.00460	0.43203
	160	*0.99977*	0.64647	0.00287	0.26657
Radbas	50	0.59211	–	0.00073	–
	100	0.82648	–	0.00174	–
	125	0.74428	–	0.00140	–
	160	0.74530	–	0.00033	–
Pureline	50	0.56077	0.55475	–	0.55238
	100	0.79305	0.78532	–	0.78703
	125	0.88666	0.87199	–	0.88104
	160	0.99938	0.93375	–	0.97054

Table 4 Samples codes related to the developed programme

Sample codes for the matching columns	Giris(:,1)=AISI1_1; Giris(:,2)=AISI1_2; Giris(:,3)=AISI1_3; Giris(:,4)=AISI1_4; Giris(:,5)=AISI2_1; Giris(:,6)=AISI2_2; …

Sample codes for the training networks	net=newff(minmax(Giris), [160160], {'logsig' 'logsig'}, 'trainscg');
	net.LW{2,1}=net.LW{2,1}*0.01;
	net.b{2}=net.b{2}*0.01;
	net.trainParam.perf='sse';
	net.trainParam.epochs=500;
	net.trainParam.goal=1e-5;
	…

Sample codes for the GUI	set(handles.unitgroup, 'SelectedObject', handles. AISI)
	run Program_AA_Son
	set(handles.deger, 'String', Ra_1);
	function steel_Callback(hObject, eventdata, handles)
	set(handles.unitgroup, 'SelectedObject', handles. AISI)
	run Program_AISI_Son
	set(handles.deger, 'String', RaAISI_1);
	…

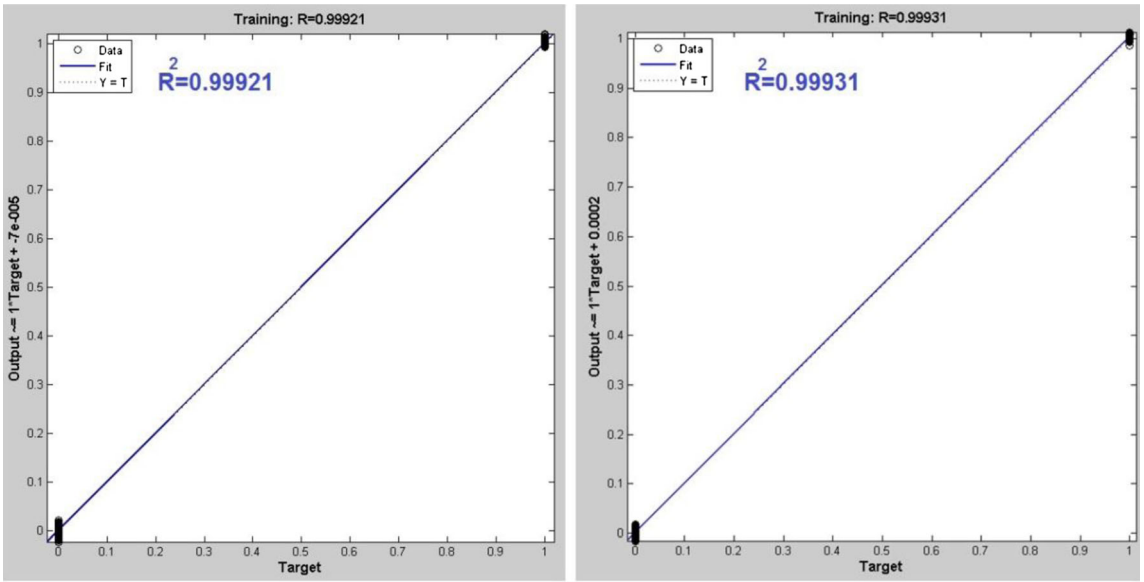

Fig. 7 Performance of the trained networks for AA 5083

image such as image major peak frequency, central power spectrum percentage, etc., with artificial neural networks. Machine vision and ANN approaches could be used for estimation and prediction of roughness of components [31]. Binary image matrices were also used as surface roughness features. The main criterion of this study was to determine the matrix size as a memory capacity of MATLAB. Therefore, after the coded software, 1,280×1,024-resolution images were evaluated at different resolutions (800×640, 700×560, 500×400, 400×320, 300×240) using ten samples for each image. These samples were used to train neural networks, and then, the trained samples were compared with their network parameters (number of iteration, R^2 value and training time). While increasing the number of the used samples, the error 'out of memory' was received from MATLAB for some resolutions (800×640, 700×560, 500×400, 400×320). Therefore, the best performance was obtained from 300×240-resolution images, and these images were selected to train networks. The selected resolution had 300 pixels in rows and 240 pixels in columns. This image size (300×240) was converted into binary format in MATLAB and was transformed into the matrix with 72,000 pixels (Fig. 5).

In Fig. 5, the process converted images into a binary file format, and all surface images added each other as binary

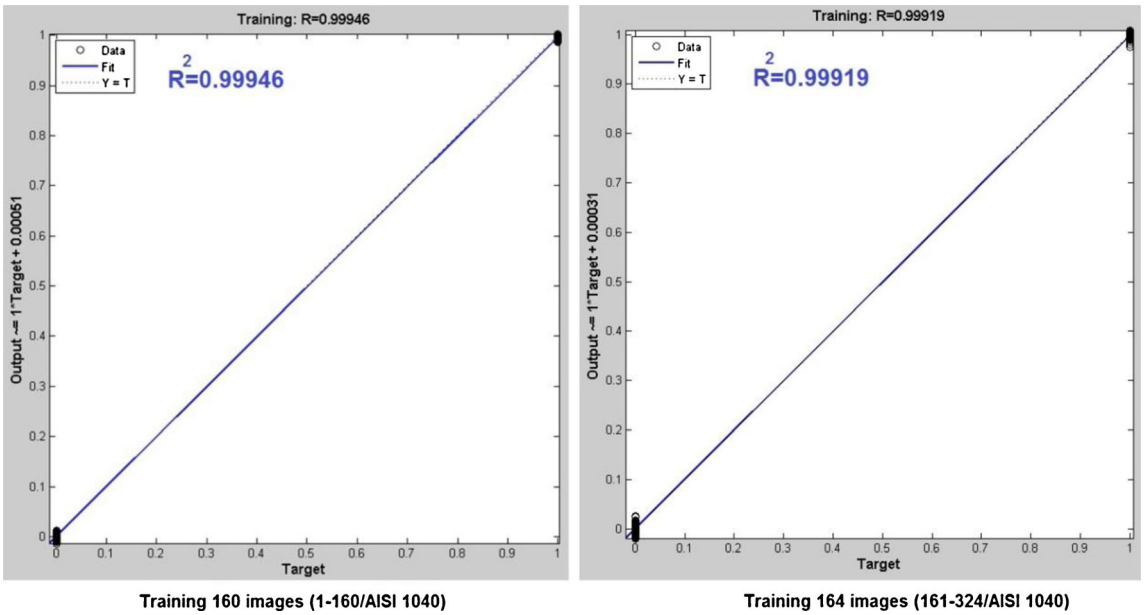

Fig. 8 Performance of the trained networks for AISI 1040

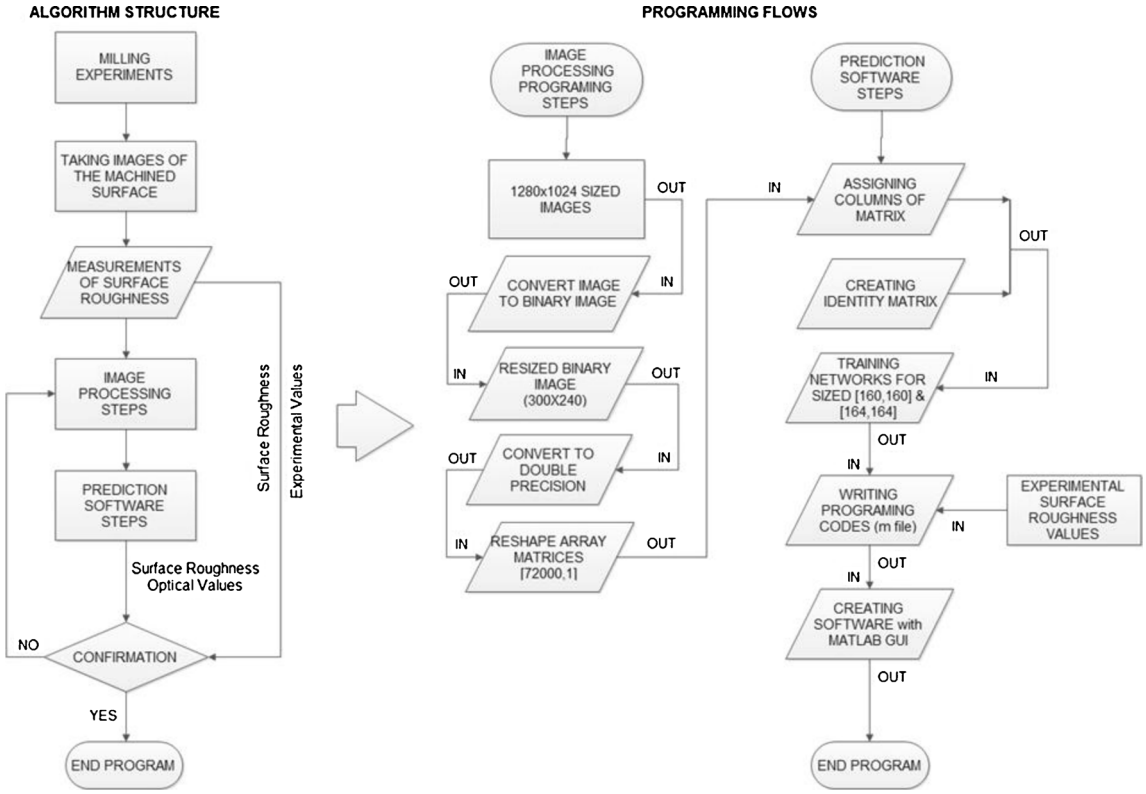

Fig. 9 The algorithm structure for developing programme and programming flows

codes are shown. Images were evaluated by dividing into two groups as 160 and 164, taking into account the maximum virtual memory of the MATLAB. As a first step, the first group consisting from 1 to 160 images was processed, and 72,000×1-sized image matrices combining side by side and 72,000×160-sized first-portion matrices were created. The remaining images from 161 up to 324 were processed in the same way, and the images created 72,000×164-sized second-portion matrices. While combining the location of each image matrix to be introduced in the programme, image name was matched with location of matrix. In addition, 160×160- and 164×164-sized unit matrices were also created to train networks. After these processes, a total of four artificial neural networks were obtained (72,000×160 and 72,000×164 for AISI 1040 and 72,000×160 and 72,000×164 for AA 5083).

3.2 Training networks

In total, four pieces of networks for two materials were trained. Before the training networks, pretest was applied to

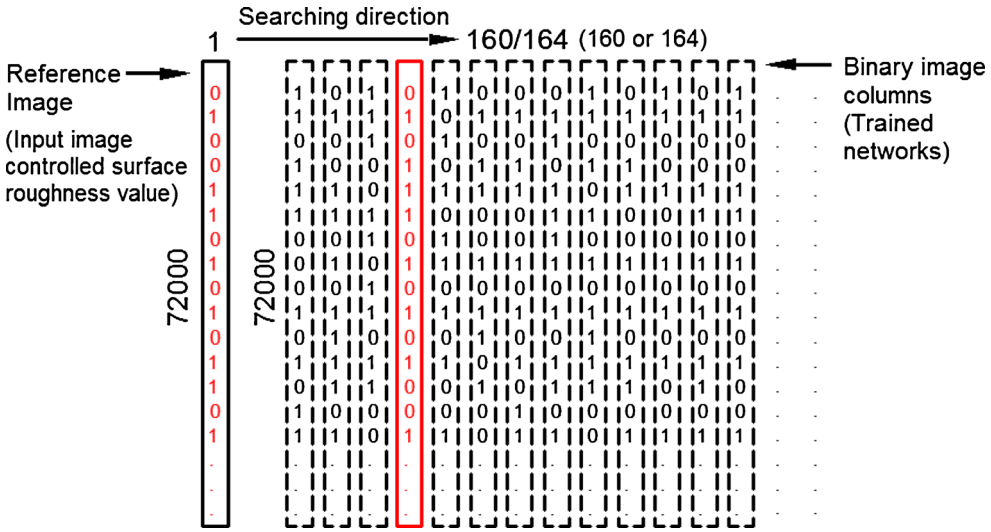

Fig. 10 Searching input image to find its similar image in learned networks

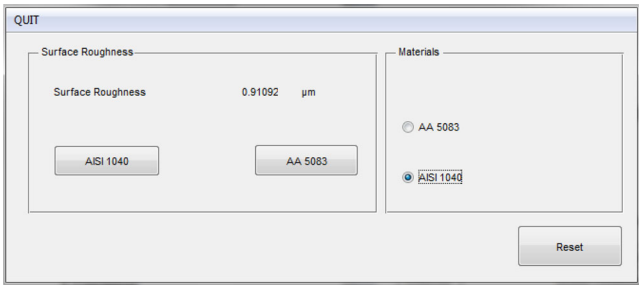

Fig. 11 The interface of developed programme

select the appropriate training algorithms and to transfer functions. In this study, the used neural network structure for the processed images is shown in Fig. 6.

The first 160 pieces of images of the two materials were used. Regression values were compared with three different transfer functions, four different numbers of neurons and four different training algorithms (Tables 2 and 3). As a result of these comparisons, log-sigmoid (logsig) transfer function and scaled conjugate gradient (SCG) back propagation algorithm were selected as network parameters for both materials.

In Tables 2 and 4, SCG back propagation, conjugate gradient back propagation with Powell-Beale restarts (CGB), gradient descent back propagation (GD) and conjugate gradient back propagation with Fletcher-Reeves updates (CGF) were selected as training algorithms. Coefficients of determination (R^2) for the material images of AA 5083 and AISI 1040 were 0.99921 and 0.99977, respectively (Table 2). Therefore, SCG training algorithm, the maximum neurons and logsig transfer function were selected to use in training networks. Network performance results of AA 5083 and AISI 1040 materials for the trained networks according to the selected network parameters are shown in Figs. 7 and 8.

3.3 Improving a prediction programme

In the stage of programme development, the algorithm structure was adapted as shown in Fig. 9, and samples' codes for this programme are shown in Table 4.

After the experiments, the measured surface roughness values and images taken from material surfaces were used in preparation of the prediction programme. Moreover, two different algorithms were coded for two materials with MATLAB m-file programming editor. In the written codes for algorithm, the obtained values for the stylus technique were matched with the position of the relevant images.

When the first command of the programme is executed, it writes the virtual memory reading trained networks in the background for the related material. The programme reads the image from the defined file location, and the 1,280×1,024-resolution image is firstly converted into binary format and then is changed into 300×240 resolution and, finally, into a single-column matrix, which is named as reference image, having 72,000×1 size. This single-column matrix file is compared with the learned network models in the image matrices, and the compliance status is checked. As an outcome, the programme gives a value between 0 and 1 (0–100 %). For example, if a result gives a value of 0.987, the evaluated image is similar to the corresponding column as 98.7 % (Fig. 10). The programme performs this search along the searching direction, and two artificial neural network files are prepared

Table 5 The comparison of experimental and programme surface roughness values for AISI 1040 material

Exp.		Cutting parameters				Surface roughness values		
No.	Measure	Cutting tools	Cutting speed (m/min)	Feed rate (mm/tooth)	Cutting depth (mm)	Exp. values (µm)	Programme values (µm)	Delta (µm)
72	3	TiALN	180	0.3	0.9	0.77	0.769	0.001
81	2	TiALN	220	0.3	0.9	0.89	0.888	0.002
80	1	TiALN	220	0.3	0.6	0.62	0.619	0.001
56	2	TiALN	160	0.1	0.6	1.47	1.470	–
58	1	TiALN	160	0.15	0.3	2.49	2.486	0.004
49	3	TiN-TiCN-Al_2O_3	220	0.15	0.3	2.47	2.471	0.001
45	2	TiN-TiCN-Al_2O_3	180	0.3	0.9	1.80	1.798	0.002
45	3	TiN-TiCN-Al_2O_3	180	0.3	0.9	1.84	1.840	–
50	4	TiN-TiCN-Al_2O_3	220	0.15	0.6	2.51	2.511	0.001
42	1	TiN-TiCN-Al_2O_3	180	0.15	0.9	3.06	3.059	0.001
26	1	UC	220	0.3	0.6	1.39	1.385	0.005
21	4	UC	220	0.1	0.9	1.30	1.295	0.005
19	1	UC	220	0.1	0.3	1.40	1.398	0.002
1	1	UC	160	0.1	0.3	1.28	1.275	0.005
14	3	UC	180	0.15	0.6	1.51	1.511	0.001

Table 6 The comparison of experimental and programme surface roughness values for AA 5083 material

Exp.		Cutting parameters				Surface roughness values		
No.	Measure	Cutting tools	Cutting speed (m/min)	Feed rate (mm/tooth)	Cutting depth (mm)	Exp. values (μm)	Software values (μm)	Delta (μm)
81	2	TiB2	650	0.25	0.25	0.69	0.691	0.001
60	1	TiB2	450	0.12	0.25	0.39	0.392	0.002
56	2	TiB2	450	0.08	0.12	0.33	0.333	0.003
67	1	TiB2	550	0.12	0.08	0.3	0.302	0.002
72	2	TiB2	550	0.25	0.12	0.43	0.430	–
52	4	TiALN	650	0.25	0.08	0.60	0.601	0.001
47	2	TiALN	650	0.08	0.12	0.33	0.330	–
35	3	TiALN	450	0.25	0.12	0.73	0.732	0.002
36	3	TiALN	450	0.25	0.25	0.65	0.652	0.002
44	3	TiALN	550	0.25	0.12	0.53	0.532	0.002
22	4	UC	650	0.12	0.08	0.29	0.292	0.002
19	1	UC	650	0.08	0.08	0.27	0.271	0.001
3	3	UC	450	0.08	0.25	0.22	0.221	0.001
15	4	UC	550	0.12	0.25	0.37	0.371	0.001
11	3	UC	550	0.08	0.12	0.32	0.321	0.001

for the relevant material. In this search, MATLAB holds the matching highest value as a temporary variable. Finally, this value is multiplied with the experimentally measured value of the roughness of the image of the corresponding column, and the obtained surface roughness value is displayed as an output on the screen (Fig. 11). The programme uses the following equation for this process:

$$Ra_{\text{img}} = C_{\text{img}} R_{\text{sty}} \quad (1)$$

where C_{img} is the image matching ratio ($0 < C_{\text{img}} < 1$), R_{sty} is the experimentally measured value with surface roughness device, and Ra_{img} is roughness value obtained from the surface image.

4 Result and discussion

4.1 Programme tested

At the end of the study, the experimental surface roughness values were compared with the programme values to test the accuracy of the programme and developed algorithm structure. Experimental values obtained from the first experiment performed to train networks were compared with the programme values shown in Tables 5 and 6. The experimental values were randomly selected as 15 pieces within the 81 pieces of experiments. The different cutting parameters were taken into account in these selections.

In Tables 5 and 6, UC is uncoated cutting inserts; TiN-TiCN-Al_2O_3 is multi-layer titanium nitride, titanium carbonitride and aluminium oxide-coated cutting inserts; TiALN is titanium aluminium nitride-coated cutting inserts; and TiB_2 is titanium-diboride-coated cutting inserts. Table values are ranging from 0.001 to 0.003 μm. Therefore, there is very little difference between these two values. As a result of verification, values of the developed programme were confirmed with 99.999 % confidence.

4.2 Trial experiments

In the final stage of the study, nine pieces of experiments were conducted using different cutting parameters for both materials (Table 7).

Table 7 Cutting parameters for the test experiments

	AISI 1040	AA 5083 H111
Cutting tools	Uncoated, CVD/TiN-TiCN-Al_2O_3, PVD/TiAlN Nano	Uncoated, PVD/TiAlN Nano, PVD/TiB_2
Cutting speeds (m/min)	100, 125, 150	200, 250, 300
Feed rates (mm/tooth)	0.05, 0.15, 0.2	0.05, 0.15, 0.2
Cutting depths (mm)	0.2, 0.4, 0.6	0.1, 0.2, 0.3

Table 8 The testing programme algorithm with different cutting parameters for the AISI 1040 material

Exp. no.	Cutting parameters				Surface roughness values		
	Cutting tools	Cutting speed (m/min)	Feed rate (mm/tooth)	Cutting depth (mm)	Exp. values (μm)	Software values (μm)	Delta (μm)
1	TiALN	100	0.05	0.2	2.59	2.558	0.030
2	TiALN	100	0.05	0.4	2.50	2.678	0.180
3	TiALN	100	0.05	0.6	2.66	2.533	0.128
4	TiN-TiCN-Al_2O_3	125	0.15	0.2	3.29	2.528	0.763
5	TiN-TiCN-Al_2O_3	125	0.15	0.4	3.15	2.490	0.655
6	TiN-TiCN-Al_2O_3	125	0.15	0.6	3.05	3.046	0.004
7	UC	150	0.2	0.2	1.46	1.850	0.390
8	UC	150	0.2	0.4	1.51	1.503	0.005
9	UC	150	0.2	0.6	1.47	1.013	0.452

In test experiments, 72 pieces of surface roughness measurements and 72 pieces of surface images were obtained. These experiments experimentally measured four surface roughness values, and surface images were taken from material surface for each measurement. Finally, average surface roughness values obtained from the surface roughness device and values of the prediction programme were compared with each other. The results of the average experimental and programme values are shown in Tables 8 and 9.

Changing the cutting parameters is very important in obtaining different surface roughness values, because there are more than one parameter that affect the surface roughness [32]. Consequently, parameters in the last test were selected as different from the initial cutting parameters, and then, the last test results were obtained from the prediction programme. The achieved surface roughness differences for average values were greater than those of the first test as shown in Fig. 12.

In Fig. 12, the comparison of the last test results is given for both materials. The minimum differences were determined in AISI 1040 steel. Hardness of the AISI 1040 material is 149 HB (Brinell), and it is harder than aluminium material [33]. Therefore, surface roughness values obtained from AISI 1040 material were larger than the others, and the rougher surface image gave a better result. On the other hand, AA 5083 is also highly resistant to be attacked by seawater and industrial chemical environments, and it is used in the shipbuilding, mine skips and cages, pressure vessels, rail cars, vehicle bodies and tip truck bodies. The hardness of AA 5083 material is 75 HV (Vickers). Since its material structure has softer than AISI 1040 material, and its surface lines are not obvious [34–36].

The quality of surface roughness significantly affects many machining operations and manufacturing processes [37–40]. Contact techniques to measure surface roughness such as stylus technique damages the machined surfaces and ruins surface quality after the measurement. Measurement techniques can be classified into two categories according to whether or not the measuring probe touches the test workpiece. Conventionally, the commonly used method in an industrial environment is the direct method through a profile meter or a measuring stylus. Even if the stylus device is still considered to be the accepted standard for measurement of surface roughness, the method has several disadvantages. The non-contact methods may present

Table 9 The testing programme algorithm with different cutting parameters for the AA 5083 material

Exp. no.	Cutting parameters				Surface roughness values		
	Cutting tools	Cutting speed (m/min)	Feed rate (mm/tooth)	Cutting depth (mm)	Exp. values (μm)	Software values (μm)	Delta (μm)
1	TiB_2	200	0.05	0.1	0.71	0.551	0.159
2	TiB_2	200	0.05	0.2	0.65	0.941	0.296
3	TiB_2	200	0.05	0.3	0.80	0.592	0.209
4	TiN	250	0.15	0.1	0.46	0.472	0.009
5	TiN	250	0.15	0.2	0.44	0.450	0.010
6	TiN	250	0.15	0.3	0.51	0.762	0.249
7	UC	300	0.2	0.1	0.47	0.611	0.141
8	UC	300	0.2	0.2	0.42	0.684	0.269
9	TiB_2	300	0.2	0.3	0.41	0.563	0.150

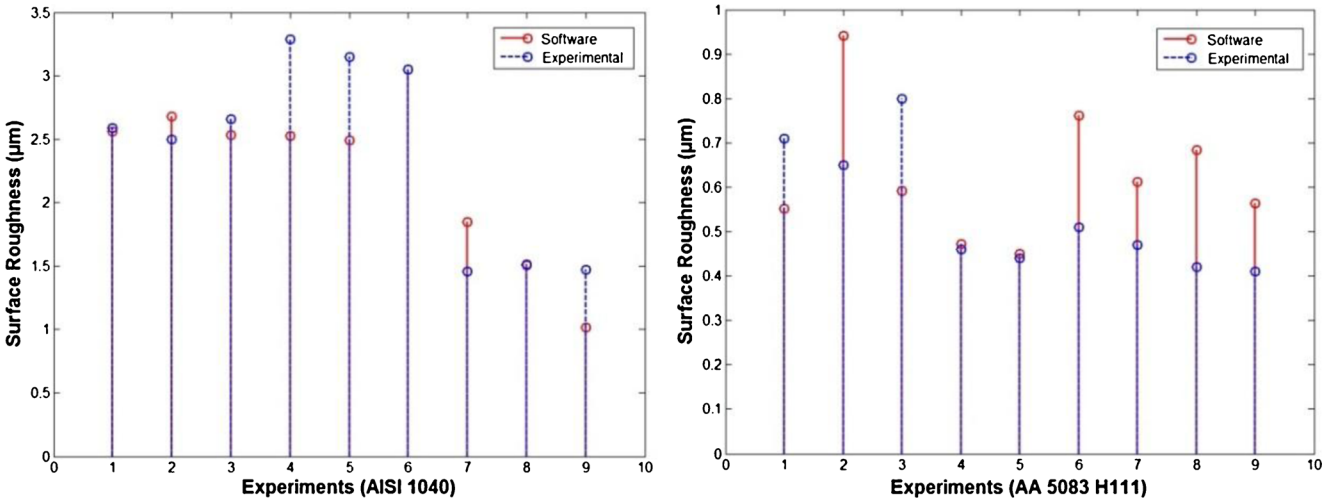

Fig. 12 The comparisons of test results for two materials

an alternative to permit the surface roughness to be measured rapidly and with an acceptable accuracy. One of the most promising non-contact methods, with regard to speed and accuracy, is the computer vision technique [41–44]. Especially, when robotic technology is adapted to the manufacturing process, artificial vision and image processing methods provide practical solutions for these areas.

5 Conclusions

In this study, a prediction programme was developed for the measurement of surface roughness as a non-contact method, using two materials for the process. The selected materials were machined using different cutting parameters affecting the surface roughness in a CNC milling machine. The obtained surface images were processed and used in training artificial neural networks. A programme was created in MATLAB to measure surface roughness of the images obtained from machined surfaces and to use artificial neural networks in the algorithm. In final stages of this study, test experiments were performed, and the following steps were completed:

- In determining the matrix size of binary images used in training networks, direction of the black and white lines on the surface image is an important criterion. Selection in the outnumber direction of these lines extended parallel to the horizontal direction increases the recognition performance of the training network.
- The best results were obtained from 300×240-resolution images.
- For the training networks, log-sigmoid function was selected as transfer function, scale conjugate gradient (SCG) algorithm was used as training algorithm, and the maximum number of neurons was selected in training networks.
- Performance of the trained networks was achieved as an average of 99.926 % for AA 5083 aluminium and as an average of 99.932 % for AISI 1040 steel.
- When test results obtained from the first images were compared with experimental results, they confirmed each other in a rate of 99.999 %.
- Even if the differences of surface roughness in test results for both materials are close, the best result is achieved by the AISI 1040 material. Therefore, when the surface roughness increases, better results are obtained by the prediction programme.

The degree of accuracy of the programme decreased in different cutting parameters. Better results may be achieved with the new experiments and by the new network learning ability. Furthermore, the conducted tests for different materials can improve further learning algorithm of the programme. Behaviour of the programme in different cutting parameters can be increased again by using a 300×240-resolution image in the training network. For this condition, decreasing the number of images used for training network will suffice. In future studies, the programme performance can be enhanced with the new experiments and studies of new materials. Additionally, this research by adapting a robot arm system can be evaluated in a larger study, and the used method and the created algorithm structure will benefit the new studies on non-contact systems. In this study, the use of the machined surface obtained from optic microscope and the developed algorithm structure for other machining processes such as turning and grinding are potential areas for future research.

Acknowledgments This project is supported by Düzce University Research Fund Project Number 2012.06.06.120. The author would like to thank the Department of Scientific Research Projects, Düzce University; Düzce, Turkey, for financially supporting this research.

References

1. Stachowiak GW, Batchelor AW, Stachowiak GB (2004) Experimental methods in tribology. Tribology Series Vol. 44 Elsevier, Netherlands
2. Bewoor AK, Kulkarni VA (2009) Metrology & measurement. McGraw-Hill, New Delhi
3. Yilbas Z, Hasmi MSJ (1999) Surface roughness measurement using an optical system. J Mater Process Technol 88:10–22
4. Jeyapoovan T, Murugan M (2013) Surface roughness classification using image processing. Measurement 46:2065–2072
5. Dhanasekar B, Ramamoorthy B (2010) Restoration of blurred images for surface roughness evaluation machine vision. Tribol Int 43: 268–276
6. Dhanasekar B, Mohan NK, Bhaduri B, Ramamoorthy B (2008) Evaluation of surface roughness based on monochromatic speckle correlation using image processing. Prec Eng 32:196–206
7. Nwaogu UC, Tiedje NS, Hansen HN (2013) A non-contact 3D method to characterize the surface roughness of castings. J Mater Process Technol 213:59–68
8. Quinsat Y, Tournier C (2012) In situ non-contact measurements of surface roughness. Prec Eng 36:97–103
9. Fuh Y-K, Hsu KC, Fan JR (2012) Roughness measurement of metals using a modified binary speckle image and adaptive optics. Optics Lasers Eng 20:3112–316
10. Laopornpichayanuwat W, Visessamit J, Tianprateep M (2012) 3-D surface roughness profile of 316-stainless steel using vertical scanning interferometry with a superluminescent diode. Measur 40:2400–2406
11. Kiran M, Ramamoorthy B, Radhakrishnan V (1998) Evaluation of surface roughness by vision system. Int J for Mach Tools Manufac 38:685–690
12. Luk F, Huynh V, North W (1989) Measurement of surface roughness by a machine vision. J Phys E Scien Inst 22:977–980
13. Al Kindi GA, Baul RM, Gill KF (1992) An application of machine vision in the automated inspection of engineering surfaces. Int J of Pro Res 2:241–253
14. Tsai D-M, Chen J-J, Chen J-F (1998) A vision system for surface roughness assessment using neural networks. Int J Adv Manufac Techn 14:412–422
15. Gao Z, Zhao X (2012) Roughness measurement of moving weak-scattering surface by dynamic speckle image. Opt Las Eng 50:668–677
16. Fuh Y-K, Hsu KC, Fan JR (2012) Roughness measurement of metals using a modified binary speckle image and adaptive optics. Optics Las Eng 50:312–316
17. Hamed AM, El-Ghandoor H, El-Diasty F, Saudy M (2004) Analysis of speckle images to assess surface roughness. Optics Laser Techn 36:249–253
18. Kayahan E, Oktem H, Hacizade F, Nasibov H, Gundogdu O (2010) Measurement of surface roughness of metals using binary speckle image analysis. Trib Int 43:307–311
19. Persson U (2006) Surface roughness measurement on machined surfaces using angular speckle correlation. J Mater Process Techn 180:223–238
20. Meireles JB, Da Silva L, Caetano DP, Huguenin JAO (2012) Effect of metallic surface roughness on the speckle pattern formation at diffraction plane. Opt Las Eng 50:1731–1734
21. Dutta S, Datta A, Das Chakladar N, Pal SK, Mukhopadhyay S, Sen R (2012) Detection of tool condition from the turned surface images using an accurate grey level co-occurrence technique. Prec Eng 36: 458–466
22. Gadelmawla ES (2004) A vision system for surface roughness characterization using the gray level co-occurrence matrix. NDT E Inter 37:577–588
23. Wang Z, Meng H, Fu J (2010) Novel method for evaluating surface roughness by grey dynamic filtering. Measurement 43:78–82
24. Sarma PMMS (2009) Karunamoorthy L, Palanikumar K, Roughness parameters evaluation in machining GFRP composites by PCD tool using digital image processing. J Rein Plast Comp 28:1567–1585
25. Bradley C, Wong YS (2001) Surface texture indicators of tool wear a machine vision approach. Int J Adv Manuf Techn 17:435–443
26. Kang MC, Kim JS, Kim KH (2005) Fractal dimension analysis of machined surface depending on coated tool wear. Surf Coat Techn 199:259–265
27. Krewet B, Zhang C, Kuhlenktter X (2006) Automatic classification of defects on the product surface in grinding and polishing. Int J Mach Tool Manuf 46:59–69
28. Zhang C, Zhang J (2013) On-line tool wear measurement for ball-end milling cutter based on machine vision. Comp Ind 64:708–719
29. Lim TY, Ratham MM (2012) Edge detection and measurement of nose radii of cutting tool inserts from scanned 2-D images. Opt Las Eng 20:1628–1642
30. Borysenko O, Kulyk I, Kostel S, Skordina O (2010) Binary image compression based on binomial numbers. Buletinul 62(2):1–12
31. Priya P, Ramamoorthy B (2007) The influence of component inclination on surface finish evaluation using digital image processing. Int J Mach Tools Manuc 47:570–579
32. Tekaslan Ö, Gerger N, Şeker U (2008) Determination of cutting parameters to obtain optimum cutting parameters in machining AISI 304 steels in CNC lathe machine. J Univ Dumlupınar Inst Sci 16:97–104
33. Çınar Ö, Çetiner BN, Tünçay MM, Topçu İ (2012) Comparison of mechanical properties of AISI 1040, 420, 4140, 316 steels after nitriding. Intl Iron & Steel Symp, Karabük, pp 680–686
34. Kechagias JD, Ziogas CK, Pappas MK, Ntziatzias IE (2011) Parameter optimization during finish end milling of Al alloy 5083 using robust design. Proc. of the World Cong. on Eng. (WCE 2011), London, 1-5
35. Pınar AM (2013) Optimization of process parameters with minimum surface roughness in the pocket machining of AA5083 aluminum alloy via Taguchi method. Arabian J Sci Eng 38(3):705–714
36. Kaufman JG (2000) Introduction to aluminum alloy and tempers. ASM International, USA
37. Klocke F (2011) Manufacturing processes 1: cutting. Springer, London
38. Durmuş H (2012) Optimization of multi-process parameters according to the surface quality criteria in the end milling of the AA6013 aluminum alloy. Mater Techn 46(4):383–388
39. Kadirgama K, Noor MM, Rahman MM, Rejad MRM, Haron CHC (2009) Surface roughness prediction model of 6061-T6 aluminium alloy machining using statistical method. Eur J Sci Res 25(2):250–256
40. Baharudin BTHT, İbrahim MR, İsmail N, Leman Z, Ariffin MKA, Majid DL (2012) Experimental investigation of HSS face milling to AL6061 using Taguchi method. Proc Eng 50:933–941
41. Al-Kindi GA, Shirinzadeh B (2009) Feasibility assessment of vision-based surface roughness parameters acquisition for different types of machined specimens. Img Vis Comp 27:444–458
42. Li X, Wang L, Cai N (2004) Machine-vision-based surface finish inspection for cutting tool replacement in production. Int J Prod Res 42(11):2279–2287
43. Lo S, Chiu J, Lin H (2005) Rapid measurement of surface roughness for face-milling aluminum using laser scattering and the Taguchi method. Int J Adv Manuf Technol 26(9–10):1071–1077
44. Jetley S, Selven D (1993) Applying machining vision to surface texture analysis. In: IEEE proceedings of the 36th Midwest symposium on circuits and systems 2: 1456–1459